Astron. Astrophys. 334, 1–10 (1998)

ASTRONOMY AND ASTROPHYSICS

Scale dependence of the bias investigated by weak lensing

L. van Waerbeke

Max-Planck-Institut für Astrophysik, Karl-Schwarzschild-Strasse 1, Postfach 1523, D-85740 Garching, Germany

Received 29 October 1997 / Accepted 17 February 1998

Abstract. The statistical analysis of the lensing effects coupled with the statistical analysis of the number counts is a tool to probe directly the relation between the mass and the light. In particular, some properties of the bias parameter can be investigated. The correlation between the shear of a given population of galaxies, and the number counts of a different population of galaxies along the same line of sight is calculated for the linear and the non-linear power spectra of density fluctuations for different cosmologies. The estimator R defined as the ratio of this correlation and the variance of the number counts is inversely proportional to the bias parameter. The signal-to-noise ratio of R shows a significant decrease in the non-linear regime where the number of galaxies per smoothing area is small. At these scales, the noise is dominated by the intrinsic ellipticities of the galaxies and by the shot noise, the cosmic variance playing a minor role. Hence, only galaxy samples larger than one square degree may allow a precise determination of R. Unfortunately, R is highly dependent on the cosmological model, which makes a direct measure of the bias quite difficult. However, it is showed that Rb is independent on the power spectrum and the smoothing scale, thus R is a direct measure of the inverse of the bias times a function of the cosmological parameters. From R, a new estimator $\mathcal{R}$ is defined which is only sensible to the scale dependence of the bias. It is showed that with a sample of 25 square degrees, one can measure a scale variation of the bias larger than 20% in the $1'$ to $10'$ scale range, almost independently of the cosmological parameters, the redshift distribution of the galaxies, and the power spectrum, which affect the estimate of the variation of b from $\mathcal{R}$ by less than 2%.

Key words: gravitational lensing – dark matter

1. Introduction

The statistical analysis of the weak lensing effects can be used to probe the projected mass distribution in the Universe and to constrain the cosmological parameters. The variance of the gravitational shear can be used (Blandford et al. 1991, Miralda-Escudé 1991, Kaiser 1992, Villumsen 1996a and Kaiser 1996), and both the variance and the skewness of the convergence can probe, almost independently, the slope of a power law power spectrum and the cosmological parameters (Bernardeau et al. 1997). These papers provide analytical and numerical estimates of these statistical estimators using the dominant order of the perturbation theory of the large-scale structure formation. Hence, these calculations are limited to scales larger than a few Megaparsecs[1] To take into account the fully non-linear evolution of the density contrast, Jain & Seljak (1997) calculated the variance of the shear using the non-linear evolution of the power spectrum derived by Peacock & Dodds (1996). They have shown that the signal is increased by a factor two to three, compared to the linear perturbation theory. More recently, Schneider et al. (1997) (hereafter SvWJK) calculated the variance and the skewness of the aperture mass $M_{\rm ap}$, which is defined as the convergence measured with a compensated filter. This statistic, inspired by the cluster lensing analysis (Kaiser et al. 1994, and Schneider 1996), has the nice property to be directly measurable from the shape of galaxies, while this is not the case for the convergence alone which is not observable.

The statistical analysis of the lensing effects may also be fruitfully coupled with the statistical analysis of the galaxy number counts (Kaiser 1992). Villumsen (1996b) has shown how the 2-point correlation function of very distant galaxies is changed due to lensing by the foreground structures. Basically, this magnification bias effect produces an enhancement of the correlation at small scales. Moessner & Jain (1997) extended these calculations into the non-linear power spectrum. Since the bias parameter enters explicitly in the calculations, this kind of study provides an original way to analyse the bias properties. However, they have shown that the lensing effect remains very small, even in the Hubble Deep Field (Villumsen et al. 1996). Sanz et al. (1997) made the first systematic analysis of the shear-number counts cross-correlations for different cosmological models. They have shown that, in the non-linear regime, the signal is significantly enhanced.

In a very recent paper, Schneider (1997) calculated the correlation $\langle M_{\rm ap}\mathcal{N}\rangle$ between $M_{\rm ap}$ and the galaxy number counts $\mathcal{N}$ filtered by a compensated filter. Using linear perturbation

Send offprint requests to: waerbeke@astro.obs-mip.fr

[1] Which corresponds to angular scales larger than $10'$ at a redshift of 0.4.

theory, he has shown that $\langle M_{\rm ap}\mathcal{N}\rangle$ is much easier to measure than $\langle M_{\rm ap}^2\rangle$ because the corresponding signal-to-noise ratio is increased by the correlation. Using this statistic, a signal-to-noise ratio per field of up to 0.5 is achieved, whatever the scale, while it is close to 0.1 for $\langle M_{\rm ap}^2\rangle$ at $10'$.

The aim of this paper is to focus on some properties of this aperture mass-number counts correlation at small scales, and its capability to measure the scale dependence of the bias parameter for a given redshift distribution of the background sources and the foreground galaxies. The $\langle M_{\rm ap}\mathcal{N}\rangle$ statistic as calculated in Schneider (1997) will be used, but the calculations will be extended into the non-linear regime to the scale of $1'$, for a variety of cosmological models. From an estimate of the signal-to-noise ratio, it is shown how the scale dependence of the bias parameter may be measured with reasonable accuracy for a wide range of scales ($1'$ to $10'$ for a survey of 25 square degrees), irrespective of the assumed cosmological model. This provides a way to probe how the bias varies with scale.

Sect. 2 presents a summary of the $M_{\rm ap}, \mathcal{N}$ and $M_{\rm ap}\mathcal{N}$ statistics. A new compensated filter is introduced, which permits simple analytical calculations in real and Fourier space. In Sect. 3, the correlation $\langle M_{\rm ap}\mathcal{N}\rangle$ is calculated in the non-linear regime, as well as its signal-to-noise ratio per field. In Sect. 4, a new statistical estimator is defined, which is able to probe the scale dependence of the bias. The measurability of this estimator is discussed in the light of the previous signal-to-noise analysis.

2. Statistics with compensated filters

In SvWJK, the aperture mass $M_{\rm ap}$ within a circular radius $\theta_{\rm c}$ is defined,

$$M_{\rm ap}(\theta_{\rm c}) = \int_0^\infty {\rm d}^2\vartheta U(\vartheta)\kappa(\boldsymbol{\vartheta}), \tag{1}$$

where $\kappa(\boldsymbol{\vartheta})$ is the convergence at the angular position $\boldsymbol{\vartheta}$, and $U(\vartheta)$ is the compensated filter,

$$U(\vartheta) = \frac{(l+2)^2}{\pi\theta_{\rm c}^2}\left[1-\left(\frac{\vartheta}{\theta_{\rm c}}\right)^2\right]^l\left[\frac{1}{l+2}-\left(\frac{\vartheta}{\theta_{\rm c}}\right)^2\right], \tag{2}$$

and $U(\vartheta) = 0$ if $\vartheta > \theta_{\rm c}$. l is an integer parameter, and $\theta_{\rm c}$ is the scale of smoothing. The aperture mass is related to the tangential part of the observable shear $\gamma_{\rm t}$,

$$M_{\rm ap}(\theta_{\rm c}) = \int_0^\infty {\rm d}^2\vartheta Q(\vartheta)\gamma_{\rm t}(\boldsymbol{\vartheta}), \tag{3}$$

where $Q(\vartheta) = \frac{2}{\vartheta^2}\int_0^\vartheta d\vartheta'\vartheta' U(\vartheta') - U(\vartheta)$ (Kaiser et al. 1994). The compensated filters cut-out the power at the scale $\theta_{\rm c}$, which leads to narrow filters in the Fourier space, well-localized around a particular frequency. However, in SvWJK, the filters $U(\vartheta)$ and $Q(\vartheta)$ are defined on a compact space ($U(\vartheta) = Q(\vartheta) = 0$ if $\vartheta > \theta_{\rm c}$), which produces oscillations in Fourier space, and leads to moderately difficult analytical and numerical calculations. A new compensated filter is introduced here, with a non-compact definition range, but with a sufficiently fast decrease such that it can be considered as a compact filter for the practical use,

$$U(\vartheta) = \frac{1}{{\theta_{\rm c}}^2}\left(1-4\frac{\vartheta^2}{{\theta_{\rm c}}^2}\right)\ \exp\left(-4\frac{\vartheta^2}{{\theta_{\rm c}}^2}\right), \tag{4}$$

and $Q(\vartheta) = \frac{4}{{\theta_{\rm c}}^2}\frac{\vartheta^2}{{\theta_{\rm c}}^2}\ \exp\left(-4\frac{\vartheta^2}{{\theta_{\rm c}}^2}\right)$. The 2-D Fourier transform of U is,

$$\frac{1}{2\pi}\int {\rm d}^2\vartheta\, U(\vartheta)\, e^{{\rm i}\mathbf{s}\cdot\boldsymbol{\vartheta}} =$$

$$\frac{1}{128}s^2\theta_{\rm c}^2\ \exp\left(-\frac{s^2\theta_{\rm c}^2}{16}\right) =: I\left(\frac{s\theta_{\rm c}}{4}\right). \tag{5}$$

Thus $I(\eta) = \frac{1}{8}\eta^2\, e^{-\eta^2}$ which peaks at $\eta = 1$. In Fourier space, both filters (2) and (4) peak at $s \simeq 4/\theta_{\rm c}$ and they have the same width. Fig. 1 displays these two filters and the square of their 2-D Fourier transform.

The filter U defined as (4) belongs to the family of wavelets. Note that it would be ideal to use wavelets, which are much more localized in the Fourier space, to probe accurately the power spectrum of the projected mass distribution. Unfortunately, for our particular case, the real space filter of most of the wavelets oscillates too rapidly to be sampled enough by the discrete distribution of the galaxies. The filter (4) seems to be a good compromise, and it is used for this work.

In SvWJK, the dispersion of $M_{\rm ap}(\theta_{\rm c})$ is calculated to be

$$\langle M_{\rm ap}^2(\theta_{\rm c})\rangle\ =\ \frac{9\pi}{2}\left(\frac{H_0}{c}\right)^4\Omega^2\int_0^{w_H}{\rm d}w\,\frac{g^2(w)}{a^2(w)}\times \int {\rm d}s\, s\, P\left(\frac{s}{f_K(w)}, w\right)\, I^2(s\theta_{\rm c}), \tag{6}$$

where $w(z)$ is the comoving distance to a redshift z (and $w_H = w(\infty)$), f_K is the comoving angular diameter distance, and P is the time-evolving 3-D power spectrum. Ω is the density parameter, and a is the cosmic expansion factor. The function $g(w) = \int_w^{w_H}{\rm d}w'\, p_{\rm b}(w')\, f_K(w'-w)/f_K(w')$ depends on the redshift distribution of the sources $p_{\rm b}(w)\,{\rm d}w = \tilde{p}_{\rm b}(z)\,{\rm d}z$.

The aperture mass $M_{\rm ap}$ should now be correlated with a distribution of galaxies along the same line of sight. From a practical point of view, it is easier to measure the redshift of the nearest galaxies, and in the following we assumed that the number counts are done in a foreground distribution of galaxies, but it is worth to note that in general, this restriction is not necessary. Following the standard bias theory, the galaxy density contrast $\delta_{\rm g}$ is related to the mass density contrast δ,

$$\delta_{\rm g} = b\,\delta. \tag{7}$$

The expected number density contrast of galaxies in the direction $\boldsymbol{\vartheta}$ is then

$$\Delta n_g(\boldsymbol{\vartheta}) = \frac{N(\boldsymbol{\vartheta})-\bar{N}}{\bar{N}} = b\int {\rm d}w\, p_{\rm f}(w)\,\delta(f_K(w)\boldsymbol{\vartheta}, w), \tag{8}$$

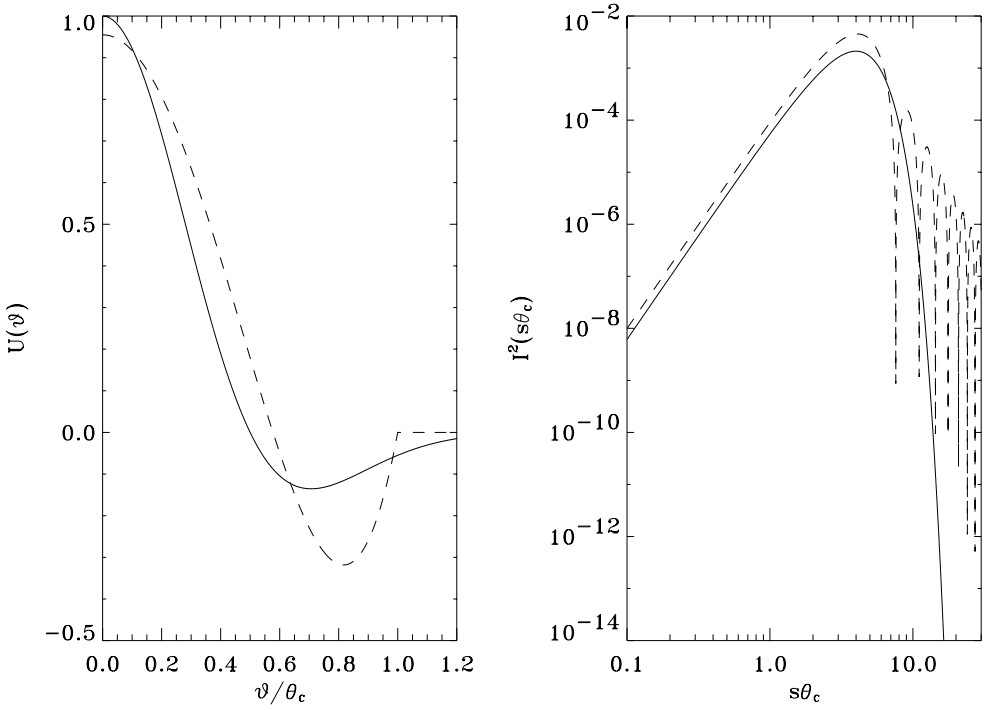

Fig. 1. On the left, the filters (2) (dashed line, for $l = 1$) and (4) (solid line). On the right, their 2-D Fourier transforms, as defined in the text.

where $\bar{N}$ is the mean number density of galaxies, $N(\boldsymbol{\vartheta})$ the number density of galaxies on the direction ϑ, and $p_{\rm f}(w)\,{\rm d}w = \tilde{p}_{\rm f}(z)\,{\rm d}z$ is the redshift distribution of the foreground galaxies. If the filtered number counts are defined as $\mathcal{N}(\theta_{\rm c}) = \int {\rm d}^2\vartheta\, U(\vartheta)\Delta n_g(\boldsymbol{\vartheta})$, the dispersion of the galaxy number counts is given by (Schneider 1997)

$$\langle \mathcal{N}^2(\theta_{\rm c})\rangle \;=\; 2\pi b^2 \int {\rm d}w \frac{p_{\rm f}^2(w)}{f_K^2(w)} \times \int {\rm d}s\; s\; P\left(\frac{s}{f_K(w)}, w\right) I^2(s\theta_{\rm c}), \qquad (9)$$

while the cross-correlation $\langle M_{\rm ap}(\theta_{\rm c})\mathcal{N}(\theta_{\rm c})\rangle$ is

$$\langle M_{\rm ap}(\theta_{\rm c})\mathcal{N}(\theta_{\rm c})\rangle \;=\; 3\pi \left(\frac{H_0}{c}\right)^2 \Omega b \times \int {\rm d}w \frac{p_{\rm f}(w) g(w)}{a(w) f_K(w)} \int \times {\rm d}s\; sP\left(\frac{s}{f_K(w)}, w\right) I^2(s\theta_{\rm c}). \qquad (10)$$

3. Numerical estimates

Now, numerical estimates of Eq. (10) are given. Four models with a CDM-like spectrum given in Bardeen et al. (1986) have been choosen. Three models are normalized to unity ($\sigma_8 = 1$), with a shape parameter $\Gamma = 0.25$. The corresponding cosmological parameters are EdS, open ($\Omega = 0.3, \Lambda = 0$) and flat ($\Omega = 0.3, \Lambda = 0.7$) Universes. Note that these models are not normalized to the cluster abundance since $\sigma_8 \simeq 0.8$ and 0.9 should be required for the open and Λ cases respectively. The fourth model is an EdS Universe with $\Gamma = 0.5$ and $\sigma_8 = 0.6$, corresponding to the cluster abundance normalization. The background and foreground populations of galaxies are assumed to follow the normalized redshift distribution

$$\tilde{p}_i(z) = \Gamma^{-1}\left(\frac{1+\alpha}{\beta}\right)\frac{\beta}{z_i}\left(\frac{z}{z_i}\right)^{\alpha}\;\exp\left[-\left(\frac{z}{z_i}\right)^{\beta}\right], \qquad (11)$$

where z_i is $z_{\rm b}$ or $z_{\rm f}$, depending on the galaxy population considered. For the background sources we assume $\alpha = 2,\ \beta = 1.5,\ z_{\rm b} = 1$, and for the foreground we take $\alpha = 5,\ \beta = 6$, with four different values for $z_{\rm f} = (0.1,\ 0.2,\ 0.3,\ 0.4)$. The foreground distribution is quite narrow, and does not overlap much with the background galaxies. We assume that it is no problem to derive $\tilde{p}_{\rm f}(z)$ from observations since the redshifts $z_{\rm f}$ are small, making these distribution observable directly from photometric redshifts, if spectroscopic redshifts are not available.

Assuming $b = 1$, Fig. 2 shows $\langle M_{\rm ap}(\theta_{\rm c})\mathcal{N}(\theta_{\rm c})\rangle^{1/2}$ versus smoothing angle $\theta_{\rm c}$ for the four cosmological models, for both the linear (thin curves) and the non-linear (thick curves) power spectra. The four plots correspond to the four different foreground redshift distributions. At small scales and for the non-linear power spectrum, the signal is strongly enhanced, by more than a factor three. This confirms that the linear evolution is negligible at these scales (Sanz et al. 1997). In Fourier space, the compensated filter peaks around $4/\theta_{\rm c}$ rather than $1/\theta_{\rm c}$ for a top hat filter. Thus, the scale at which the linear and the non-linear evolution of the structures are equal is shifted to larger scale, compare to the case of a top-hat filter (Jain & Seljak 1997). The curves are shifted towards smaller scales when the foreground galaxies are located at higher redshifts. This is due to the fact that at higher redshift, a given angular scale corresponds to a larger physical scale, where the non-linear power spectrum is closer to the linear power spectrum, and that at high redshift, the

power spectrum is less evolved than at small redshift. For the non-linear power spectrum , the peak in $\langle M_{\rm ap}(\theta_{\rm c})\mathcal{N}(\theta_{\rm c})\rangle^{1/2}$ is shifted to small scales compared to the linear power spectrum because of the transfer of power from the larger to the smaller scales (this was also observed for the $M_{\rm ap}$ statistic, see SvWJK).

Fig. 3 shows $\langle M_{\rm ap}(\theta_{\rm c})\mathcal{N}(\theta_{\rm c})\rangle^{1/2}$ versus the redshift $z_{\rm f}$ of the foreground galaxies (for $b=1$), where the redshift distribution (11) is used. The two plots correspond to $\theta_{\rm c}=1'$ (left) and $\theta_{\rm c}=10'$ (right). At scale of $1'$ the contribution of the linear evolution to the correlation is again very small. The maximum of the correlation is obtained for foreground galaxies located at relatively low redshift, compared to the mean redshift of the background galaxies ($z_{\rm b}=1$). The reason is that for a given smoothing scale, a lower redshift corresponds to a higher density contrast, which means a stronger signal. Moreover this effect is more important for the non-linear power spectrum where a *bump* is clearly seen compared to the linear power spectrum.

The same practical estimators for $M_{\rm ap}$ and N as those introduced in Schneider (1997) are used to estimate the noise of this statistic,

$$\begin{aligned}\tilde{M}_{\rm ap} &= \frac{\pi\theta_{\rm lim}^2}{N_{\rm b}}\sum_{i=1}^{N_{\rm b}} Q(|\vartheta_i|)\epsilon_{ti}\\ \tilde{N} &= \frac{1}{\bar{N}}\sum_{i=1}^{N_{\rm f}} U(|\vartheta_i|),\end{aligned} \tag{12}$$

where $\boldsymbol{\vartheta}_i$ and ϵ_{ti} are the position and the tangential component of the ellipticity of the i^{th} galaxy, $\theta_{\rm lim}$ is a radius cut of the filter (otherwise, it extends to infinity), and $N_{\rm f}$ and $N_{\rm b}$ are respectively the number of galaxies found in the foreground population, and those used for the determination of the shear, in the region limited by the radial cut. $\theta_{\rm lim}$ may be choose arbitrarly, according to Fig. 1 one could decide $\theta_{\rm lim}>2\,\theta_{\rm c}$ in the center of the whole field, and $\theta_{\rm lim}\simeq 1.2\,\theta_{\rm c}$ at the edge of the field. The dispersion of $\langle M_{\rm ap}(\theta_c)\mathcal{N}(\theta_c)\rangle$ is given by the square root of the expectation value $E\left[M_{\rm ap}^2(\theta_{\rm c})\mathcal{N}^2(\theta_{\rm c})\right]-E^2\left[M_{\rm ap}(\theta_{\rm c})\mathcal{N}(\theta_{\rm c})\right]$. The signal-to-noise is defined as the measured signal divided by the standard deviation of $\langle M_{\rm ap}(\theta_{\rm c})\mathcal{N}(\theta_{\rm c})\rangle$ obtained in the case of no correlation between $M_{\rm ap}$ and $\mathcal{N}$. This standard deviation is simply the square root of $E\left[M_{\rm ap}^2(\theta_{\rm c})\right]E\left[\mathcal{N}^2(\theta_{\rm c})\right]$. The signal-to-noise $\mathcal{S}_{\theta_{\rm c}}$ of the cross-correlation $\langle M_{\rm ap}(\theta_{\rm c})\mathcal{N}(\theta_{\rm c})\rangle$ for one field is thus (cf Schneider 1997),

$$\mathcal{S}_{\theta_{\rm c}}=\frac{\langle M_{\rm ap}(\theta_{\rm c})\mathcal{N}(\theta_{\rm c})\rangle}{\left[\langle M_{\rm ap}^2(\theta_{\rm c})\rangle+\frac{G\sigma_\epsilon^2}{2N_{\rm b}}\right]^{1/2}\left[\langle\mathcal{N}^2(\theta_{\rm c})\rangle+\frac{\tilde{G}}{N_{\rm f}}\right]^{1/2}}, \tag{13}$$

where $G=\pi\theta_{\rm lim}^2\int{\rm d}^2\vartheta Q^2(\vartheta)=0.6\left(\frac{\theta_{\rm lim}}{\theta_c}\right)^2$, $\tilde{G}=\pi\theta_{\rm lim}^2\int{\rm d}^2\vartheta U^2(\vartheta)=G$, and σ_ϵ is the dispersion of the intrinsic ellipticities of the galaxies.

Fig. 4 shows the signal-to-noise ratio given by (13). It is assumed[2] that the mean number density of the foreground galaxies is $\bar{N}\simeq 5\,{\rm gal/arcmin}^2$ and that the number density of the background galaxies is $n_{\rm b}=60\,{\rm gal/arcmin}^2$, with $\sigma_\epsilon=0.2$. We find that $\mathcal{S}_{\theta_{\rm c}}$ remains almost constant for scales $\theta_{\rm c}>10'$ whatever the cosmology. This result was found by Schneider (1997) for an EdS model and a power law spectrum. Unfortunately, this is no longer valid at small scales (few arcmin), where the effect of intrinsic ellipticities and the discrete distribution of the galaxies become dominant. The increase of the signal compared to the noise is stronger in the case of the non-linear power spectrum, this is why at small scales, $\mathcal{S}_{\theta_{\rm c}}$ is always higher for a non-linear power spectrum. The redshift of the foreground galaxies is also an important factor, we see that $\mathcal{S}_{\theta_{\rm c}}$ decreases significantly if $z_{\rm f}=0.1$. Fortunately, even with this dramatic decrease of $\mathcal{S}_{\theta_{\rm c}}$ at small scales, it remains higher than for the $\langle M_{\rm ap}^2\rangle$ statistic, where $\mathcal{S}_{\theta_{\rm c}}$ is close to 0.1 (SvWJK). As quoted in Schneider (1997), this makes the background-foreground correlation statistic more interesting for the detection of cosmic shear, in particular if the size of the catalogues used for lensing analysis are not larger than a few square degrees.

[2] This roughly corresponds to 4 hours exposure on a 4 meter telescope in the B band (Tyson 1988).

4. Investigation of some bias properties

Eq. (10) provides that a direct estimate of the bias parameter, provided the cosmological model is known. To investigate the bias properties, we define the ratio R

$$R=\frac{\langle M_{\rm ap}(\theta_{\rm c})\mathcal{N}(\theta_{\rm c})\rangle}{\langle\mathcal{N}^2(\theta_{\rm c})\rangle}, \tag{14}$$

which is independent of the normalization of the power spectrum. It is easy to show from (10) and (9) that in the case of a power law power spectrum $P(k)\propto k^n$, R is independent of scale,

$$R=\frac{3}{2}\left(\frac{H_0}{c}\right)^2\frac{\Omega}{b}\frac{\int{\rm d}w\frac{p_{\rm f}(w)g(w)D_+^2(w)}{a(w)f_K^{(1-n)}(w)}}{\int{\rm d}w\frac{p_{\rm f}^2(w)D_+^2(w)}{f_K^{(2-n)}(w)}}, \tag{15}$$

where $D_+(w)$ is the linear growth factor of the density perturbations. This property offers the possibility to measure the scale dependence of the bias (if it exists) because $R\propto 1/b$, and R is a measurable quantity. A measure of the bias itself is also possible, but it requires the knowledge of the cosmological parameters, and the slope of the power spectrum. Moreover, the background and foreground redshift distributions have to be known. Thus only the effects of a scale dependent bias will be investigated here.

The true power spectrum is certainly not a power law and R may depend in a complicated way on the cosmology, the smoothing scale, the power spectrum, and the redshift distributions. All these things coupled together, Rb is no longer scale-independent. Fortunately, the compensated filter U is very narrow in Fourier space, and even for a general power spectrum, it is fully justified to approximate it locally as a power law, with a local effective slope $n_{\rm eff}$. Furthermore, since in practice one can select the foreground galaxies in a narrow redshift range,

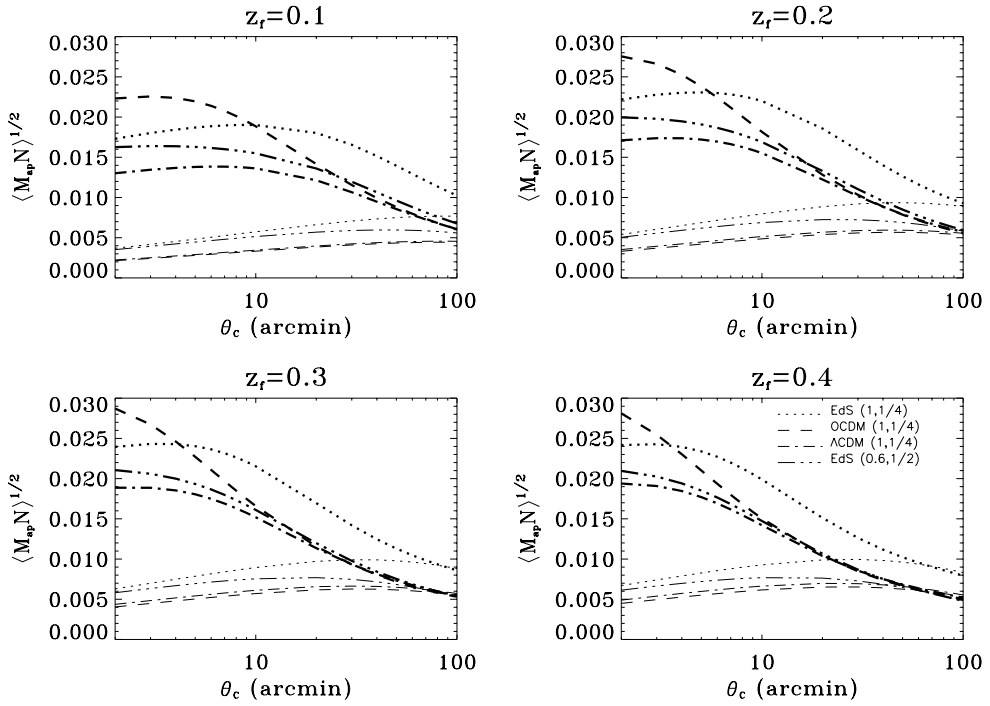

Fig. 2. The values of $\langle M_{\rm ap}(\theta_{\rm c})\mathcal{N}(\theta_{\rm c})\rangle^{1/2}$ versus the smoothing scale are shown. The case of a non-linear power spectrum is plotted in thick lines using the Peacock & Dodds formula. The thin lines show the linear power spectrum. Different types of lines correspond to different cosmologies. The top-left, top-right, bottom-left, bottom-right plots correspond to the foreground redshift distribution according to (11) with $z_{\rm f} = (0.1,\ 0.2,\ 0.3,\ 0.4)$. For the background galaxies we choose $z_{\rm b} = 1$. The cosmological models are $\Omega = 1,\ \Lambda = 0,\ \sigma_8 = 1,\ \Gamma = 0.25$ (EdS (1,1/4)), $\Omega = 0.3,\ \Lambda = 0,\ \sigma_8 = 1,\ \Gamma = 0.25$ (OCDM (1,1/4)), $\Omega = 0.3,\ \Lambda = 0.7,\ \sigma_8 = 1,\ \Gamma = 0.25$ (ΛCDM (1,1/4)), $\Omega = 1,\ \Lambda = 0,\ \sigma_8 = 0.6,\ \Gamma = 0.5$ (EdS (0.6,1/2))

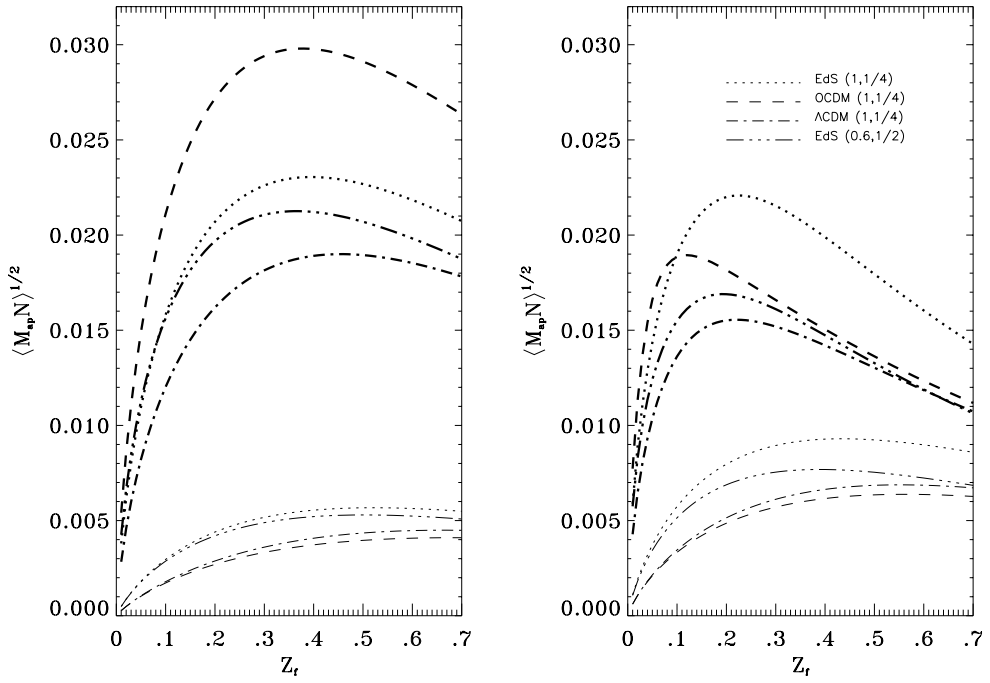

Fig. 3. The values of $\langle M_{\rm ap}(\theta_{\rm c})\mathcal{N}(\theta_{\rm c})\rangle^{1/2}$ versus the redshift of the foreground galaxies $z_{\rm f}$ given by (11) for two different smoothing scales ($\theta_{\rm c} = 1'$ on the left and $\theta_{\rm c} = 10'$ on the right), and it is assumed $b = 1$. The thick lines correspond to the non-linear power spectrum, the thin ones to the linear power spectrum.

both the redshift and wavevector integrations in (10) are very localized. Hence, the local approximation of a general power spectrum by a power law is very reasonable.

If b is only redshift dependent, this dependence can be absorbed by the function $p_{\rm f}(w)$, and R remains scale-independent. However, if b is in addition scale dependent, it means that b depends on the 3-D wavevector $\mathbf{k}$. For simplicity let us assume that the redshift and the wavevector dependences are separable. Fry and Gaztañaga (1993) proposed to model such a bias as a convolution,

$$\tilde{\delta}_{\rm g}(\mathbf{k}) = \tilde{b}(\mathbf{k})\tilde{\delta}(\mathbf{k}). \tag{16}$$

In that case, since b is not a constant, R is no longer inversely proportional to b, because it should be included in the projection effects. This drawback is avoided if the foreground redshift distribution is narrow, and if the Fourier transform of the aperture filter is narrow, such that the s integration in (10) is performed

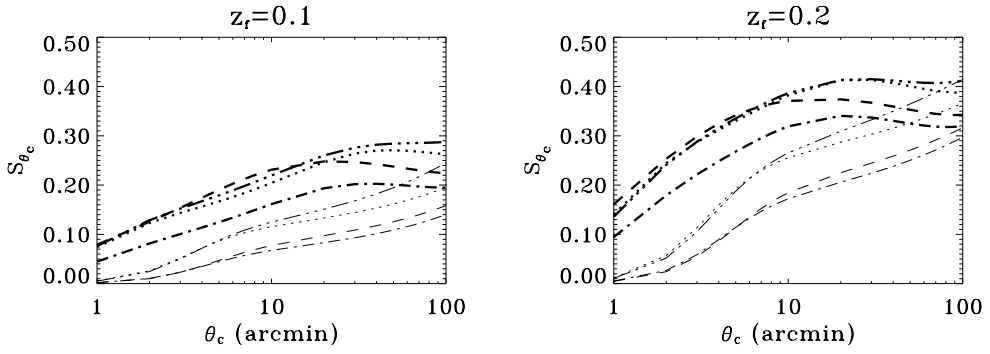

Fig. 4. Signal-to-noise ratio $\mathcal{S}_{\theta_c}$ of $\langle M_{\rm ap}(\theta_c)\mathcal{N}(\theta_c)\rangle$ as defined in the text, versus the smoothing scale, with $b = 1$. These plots show the expected signal-to-noise for one field of characteristic radius θ_c. The thick lines correspond to the non-linear power spectrum, the thin ones to the linear power spectrum. At large scale $\mathcal{S}_{\theta_c}$ obtained from the linear power spectrum can be larger than $\mathcal{S}_{\theta_c}$ of the non-linear power spectrum.

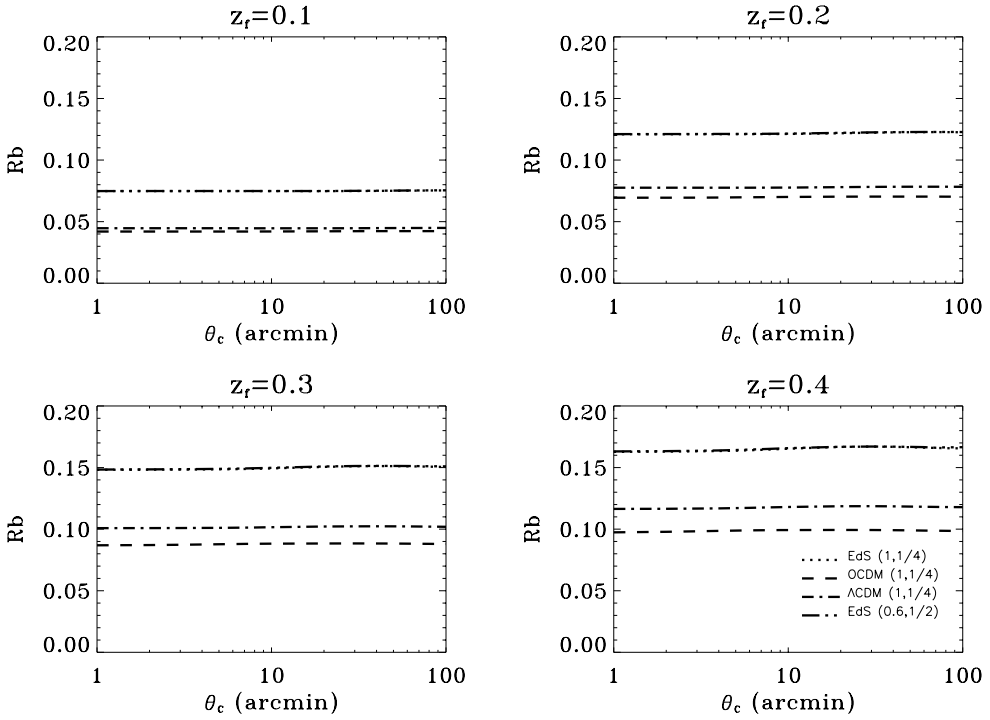

Fig. 5. The values of Rb (Eq. (15)) versus the smoothing scale are shown. The non-linear and the linear power spectrum give almost the same results, thus only the thick lines are plotted. As can be seen, the two EdS cosmological models which differ by the normalization and by the shape parameter give also the same results because R does not depend on σ_8.

on a very narrow range, and b can be approximated as "locally" independent of redshift and scale. This is the reason for choosing the foreground redshift distributions to be so narrow.

These remarks are rather phenomenological, but they illustrate what happens in the case of a general power spectrum for which R is intrinsically scale dependent. Fig. 5 shows Rb versus the smoothing scale θ_c for the cosmological models considered before. The linear and non-linear power spectra give almost the same results, thus only the thick lines corresponding to the non-linear power spectrum are shown here. The flatness of the curves is remarkable, and confirms that even for a general power spectrum, R depends weakly on scale. The amplitude depends on the cosmology, the shape of the power spectrum, as well as on the redshift distribution of the foreground and background galaxies. It is important to note that the non-linear power spectrum may also be approximated locally as a power law, because

R is independent on scale. This impressive flatness of R versus the scale for a general power spectrum should be discussed, because it is not so intuitive. Indeed, for non power-law power spectra, the effective index $n_{\rm eff}$ must be scale dependent. The very small variation of R with respect to $\theta_{\rm c}$ in Fig. 5 means that the value of the effective index has no strong influence on the value of R, in other words, the dependence of the numerator and the denominator on $n_{\rm eff}$ should nearly cancel. This is indeed the case: if a sharply peaked redshift distribution for the foreground galaxies around $z_{\rm f}$ is considered in (15), one finds

$$R \simeq \frac{3}{2}\left(\frac{H_0}{c}\right)^2 \frac{\Omega}{b}\frac{g(w_{\rm f})f_K(w_{\rm f})p_{\rm f}(w_{\rm f})}{a(w_{\rm f})\int dw\, p_{\rm f}^2(w)}. \quad (17)$$

Thus it is not surprising that R does not depends on n provided that the foreground redshift distribution is narrow. To check this assertion, three other power spectra have been tested: the Baugh & Gaztañaga (1996) power spectrum (which behaves like $\propto k^{-2}$ at large k),

$$P(k) \propto \frac{k}{[1+(k/k_{\rm c})^2]^{3/2}}, \quad (18)$$

where[3] $k_{\rm c} = 0.05\, h{\rm Mpc}^{-1}$, and two power law spectra $P(k) \propto k^n$, with $n=-1$ and $n=0$. The values of R from these three power spectra are almost the same as the values plotted in Fig. 5. The difference is always smaller than 3%, the worst case is for $n=0$, $z_{\rm f}=0.4$ for which a variation of 5% is obtained only for $\theta_{\rm c} = 100'$. These results confirm that R is independent of n at least for $n \in [-3,0]$, in addition to be independent of scale. Hence, R is a direct estimator of the bias and the cosmology, nearly independent of the power spectrum and the smoothing scale. Using other calculations of Rb for different cosmologies, and for $z_{\rm f}=0.4$, a power law fit to the Ω dependence of Rb (with a zero cosmological constant) gives

$$R \propto \frac{\Omega^{0.42}}{b}. \quad (19)$$

The proportionality constant and the exponant 0.42 should both depend on the foreground and background redshift distributions. Whether these numbers depend in a crucial way on these distributions will be investigated in a future work, but it is worth to note that Rb remains a discrimator of the bias and the cosmology, almost independent of the power spectrum and the smoothing scale.

This encouraging result is motivating for the detection of a possible variation of the bias with the scale, using the measurable quantity $\mathcal{R}$,

$$\mathcal{R} = \frac{R_{\theta_{\rm c}}}{R_{\theta_{\rm c}=1'}} = \frac{b(1')}{b(\theta_{\rm c})}, \quad (20)$$

$\mathcal{R}$ has the advantage of being only bias dependent. Fig. 6 shows $\mathcal{R}$ versus the smoothing scale $\theta_{\rm c}$. For the wide range of scales $[1', 100']$ considered here, this ratio remains very close to 1 with a variation smaller than 2% whatever the cosmological model, and whatever the redshift distribution of the foreground galaxies, provided that b is scale independent. This is the main result of this paper. It means that the degeneracy between the bias parameter and the other cosmological parameters and the power spectrum may be partially removed by choosing a particular filtering in the $\mathbf{k}$ and redshift spaces. The consequence here is to allow a measurement of the scale dependence of the bias without any knowledge of the cosmological model.

According to Bardeen et al. (1986), the bias may be redshift dependent $b \propto 1+z$. The effect of the introduction of this dependence has been calculated, and it changes the values of $\mathcal{R}$ by less than 0.001%, because $p_{\rm f}(w)$ is chosen to be sufficiently narrow; only the amplitude of R is changed, which does not affect $\mathcal{R}$. Calculations with a different power spectrum (Baugh & Gaztañaga 1996), and different redshift distributions for the background galaxies ($z_{\rm b}=0.7$ and $z_{\rm b}=1.5$) have also been performed, and it is found that the change of the shape of $\mathcal{R}$ versus $\theta_{\rm c}$ is less than 0.5% for smoothing scales larger than $20'$, and insignificant for smaller scales. Thus $\mathcal{R}$ is an estimator of the scale dependence of the bias almost independently of the redshift distribution of the background galaxies and of any hypothesis of the power spectrum and the cosmological parameters.

Next, estimates of the dispersion of $\mathcal{R}$ for a given number $N_{\theta_{\rm c}}$ of fields of size $\theta_{\rm c}$ are given. To calculate it, the dispersion of $M_{\rm ap}(\theta_{\rm c})\mathcal{N}(\theta_{\rm c})$ and of $\mathcal{N}^2(\theta_{\rm c})$ are required. The former has already been calculated (Eq. (13) and Fig. 4 give the signal-to-noise), but the latter remains difficult to estimate. However, $\langle\mathcal{N}^2(\theta_{\rm c})\rangle$ can be assumed to be known very precisely from the existing and forthcoming large galaxy catalogues[4] because the redshift of the foreground galaxies is chosen to be quite low ($z\sim 0.3$). Therefore the dispersion of $\langle\mathcal{N}^2(\theta_{\rm c})\rangle$ is neglected in estimating the dispersion of $\mathcal{R}$. If $\langle\mathcal{N}^2(\theta_{\rm c})\rangle$ is estimated from a different catalogue than the catalogue used for $\langle M_{\rm ap}(\theta_{\rm c})\mathcal{N}(\theta_{\rm c})\rangle$, then it is important to have the same selection criteria for the foreground galaxies of both catalogues. Otherwise, the bias factor in the numerator and the denominator of (15) may not be the same. The dispersion of $\mathcal{R}$ will be derived in the limit of a small correlation between $M_{\rm ap}(\theta_{\rm c})$ and $\mathcal{N}(\theta_{\rm c})$, which in fact correspond to a determination of the signal-to-noise of $\mathcal{R}$ rather than the complete calculation of the dispersion. If one observes more than one field, the signal-to-noise of $M_{\rm ap}(\theta_{\rm c})\mathcal{N}(\theta_{\rm c})$ will be reduced by a factor $\sqrt{N_{\theta_{\rm c}}}$, and if $N_{\theta_{\rm c}} \gg 1$, the dispersion of $M_{\rm ap}(\theta_{\rm c})\mathcal{N}(\theta_{\rm c})/\langle M_{\rm ap}(\theta_{\rm c})\mathcal{N}(\theta_{\rm c})\rangle$ is small compared to 1 so that the dispersion of $\mathcal{R}$ is simply

$$\sigma_{\mathcal{R}} = \sqrt{\frac{1}{N_{\theta_{\rm c}}\mathcal{S}^2_{\theta_{\rm c}}} + \frac{1}{N_{1'}\mathcal{S}^2_{1'}}} \quad (21)$$

where $\mathcal{S}_{\theta_{\rm c}}$ is the signal-to-noise of $M_{\rm ap}(\theta_{\rm c})\mathcal{N}(\theta_{\rm c})$ at the scale $\theta_{\rm c}$, given by Eq. (13). $\sigma_{\mathcal{R}}$ is derived in Appendix A.

The reason why $\mathcal{R}$ is normalized to its value at $1'$ is to minimize the error on $\mathcal{R}$. The dispersion $\sigma_{\mathcal{R}}$ is calculated by

[3] $h = H_0/100$

[4] Like the CFRS, the LCRS, the 2dF, the SDSS, the VIRMOS survey, and the EIS survey.

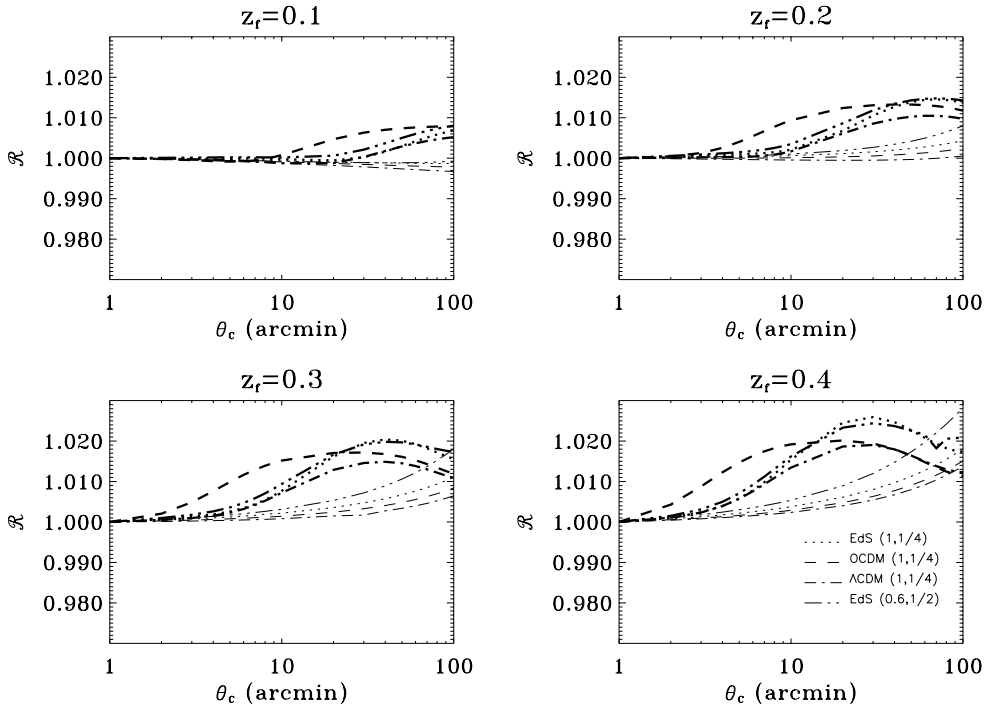

Fig. 6. The values of $\mathcal{R}$ (Eq. (20)) versus the smoothing scale are shown. The thick lines are for the non-linear power spectrum, while the thin lines are for the linear power spectrum. Whatever the cosmology, the largest variation expected for $\mathcal{R}$ is lower than about 2%, provided the bias parameter is constant with scale.

taking for $\mathcal{S}^2_{\theta_c}$ and $\mathcal{S}^2_{1'}$ the values found in Fig. 4, averaged over the four cosmological models for each smoothing scale, and for the non-linear power spectrum. Fig. 7 shows the expected error bars for a survey of 25 square-degrees. The number of fields of diameter $2\theta_c$ (in arcmin) is given by $N_{\theta_c} = 2.25 \times 10^4/\theta_c^2$ (the distance between two neighboring fields is chosen to be $2\theta_c$, see Appendix A for a discussion about the decorrelation properties of two neighboring fields), and the number densities of foreground and background galaxies are the same as above ($\bar{N} = 5$ gal/arcmin^2 and $n_b = 60$ gal/arcmin^2). We see that a variation of the bias of more than 20% over the scale interval $[1', 10']$ is detectable, but if the foreground galaxies are located around $z_f \simeq 0.1$, the error bars are larger, which is a consequence of the lower signal-to-noise in that case (see the upper left plot in Fig. 4).

A complete calculation of the cosmic variance of $\mathcal{R}$ remains to be done, but the order of magnitude of the signal-to-noise calculated here shows the feasability of the measurement of the scale dependence of the bias parameter from surveys of a few ten square degrees size.

5. Conclusion and discussion

The cross-correlation between the aperture mass and number counts for a wide range of scales $[1', 100']$, and for different cosmological models has been calculated. The non-linear evolution of the power spectrum has been taken into account. It was found that the signal is dominated by this non-linear clustering. At scales larger than about $8'$, the signal-to-noise ratio per field is ~ 0.4, close to the corresponding value calculated with the linear power spectrum. At small scales, the signal-to-noise per field decreases to $0.1 - 0.2$ at $1'$, while it is close to zero for the linear power spectrum. Moreover, a significant additional decrease of the signal-to-noise has been found when the foreground galaxies are located at very low redshift (~ 0.1).

The second part of this paper is focussed on the measurement of the scale dependence of the bias, in the light of the previous results. It has been shown that the quantity Rb, (where R is defined as the cross-correlation of the aperture mass-number counts divided by the dispersion of the number counts), is almost independent of scale. The reason for this is that the narrow filter applied in Fourier space and the assumed narrow redshift distribution of the foreground galaxies reduce considerably the range of integration over the scales and the redshifts in Eq. (10). This allows to approximate a general power spectrum as a power law, for which Rb is independent on scale. Moreover, it has been shown that Rb is almost independent of the slope of this power law, thus Rb is nearly independent of the shape of a general power spectrum, in addition to be independent on scale. R is thus a direct measure of the bias times a function which involves the cosmological parameters, and the redshift distributions of the foreground and background galaxies. The quantity $\mathcal{R}$, which is the ratio of R at two different scales is only bias dependent; it is a measure of the ratio of the bias at these two different scales. Even for a general cosmological model, $\mathcal{R}$ remains almost independent of the power spectrum (because R is also independent of it), the cosmological parameters, the redshift distribution of the foreground and background galaxies, if the bias parameter is independent of scale. It has been shown that $\mathcal{R}$ may be used to measure a pure scale dependence of the bias, and the expected signal-to-noise ratio for a survey of 25 square degrees size has been calculated. A variation of the bias of more than 20% over the scale range $[1', 10']$ is detectable from this survey, provided that the variance $\langle \mathcal{N}^2(\theta) \rangle$ of the number counts is well known (from other surveys for instance). Since

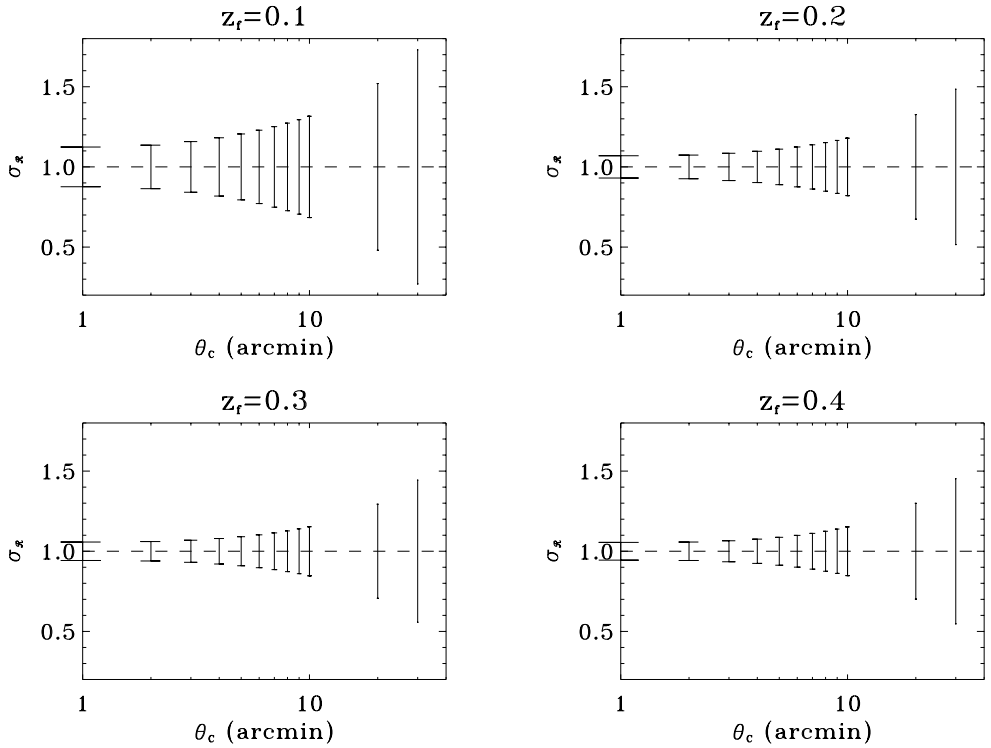

Fig. 7. The dashed line show $\mathcal{R} = 1$, and error bars are the standard deviation of $\mathcal{R}$ versus the smoothing scale. It correspond to a 25 square degrees field.

the observer has the choice to select different redshift intervals for the foreground galaxies, it is in addition possible to detect a possible redshift dependence of the variation of the bias with scale.

The method presented here allows a measure of a variation of the bias with scale if it is larger than 2% between $1'$ and $100'$. Below this limit, some residual couplings between the cosmology, the power spectrum, and the redshift distributions of the galaxies produce some variations in the curve $\mathcal{R}(\theta_{\rm c})$. However, for the largest scales considered here, it seems difficult to reach this limit in the near future because a very large survey would be required. For example, if we want a precision of $\pm\, 0.2$ on $\mathcal{R}$ at $\theta_{\rm c} = 100'$, a survey of 900 square degrees is required (with such a size, the error bars are smaller than 0.02 for scales below $10'$).

The foreground redshift distributions discussed here are available with photometric redshifts. For the shear measurement, the image quality must be good, and wide field cameras are necessary. A MEGACAM survey with 25 square degrees, UBVRI colors, and a median seeing of $0"6$ would be perfect.

Acknowledgements. I am very grateful to P. Schneider, F. Bernardeau, Y. Mellier and T. Erben for many stimulating discussions and very useful suggestions. I thank S. Charlot who kindly calculated the precise redshift number counts required for the estimation of the signal-to-noise. I am grateful to IAP for hospitality, where part of this work has made some progress, and to the *programme national de cosmologie*. This work was supported by the "Sonderforschungsbereich 375-95 für Astro-Teilchenphysik" der Deutschen Forschungsgemeinschaft.

Appendix A: evaluation of the standard deviation of $\mathcal{R}$

In this Appendix, the standard deviation of $\mathcal{R}$ is derived in the limit of small correlation between $M_{\rm ap}(\theta_{\rm c})$ and $\mathcal{N}(\theta_{\rm c})$, this gives the signal-to-noise of the estimator $\mathcal{R}$. $\mathcal{R}$ is defined in Eq. (20), which requires $R_{\theta_{\rm c}}$, defined in Eq. (14). If a number $N_{\theta_{\rm c}}$ of fields of size $\theta_{\rm c}$ are observed, the estimated value of R is,

$$\tilde{R} = \frac{\frac{1}{N_{\theta_{\rm c}}}\sum_{i=1}^{N_{\theta_{\rm c}}}\left[\tilde{M}_{\rm ap}(\theta_{\rm c})\tilde{\mathcal{N}}(\theta_{\rm c})\right]_i}{\langle\mathcal{N}^2(\theta_{\rm c})\rangle}. \tag{A1}$$

The tilde quantities always refers to the estimator of this quantity. The observable $\tilde{X}_{\theta_{\rm c}} = \frac{1}{N_{\theta_{\rm c}}}\sum_{i=1}^{N_{\theta_{\rm c}}}\left[\tilde{M}_{\rm ap}(\theta_{\rm c})\tilde{\mathcal{N}}(\theta_{\rm c})\right]_i$ is introduced. It is assumed that its signal-to-noise is simply $\mathcal{S}_{\theta_{\rm c}}\sqrt{N_{\theta_{\rm c}}}$, where $\mathcal{S}_{\theta_{\rm c}}$ is the signal-to-noise of $\tilde{M}_{\rm ap}(\theta_{\rm c})\tilde{\mathcal{N}}(\theta_{\rm c})$ in one field of size $\theta_{\rm c}$ (see Eq. (13)). This assumption implicitly neglect the correlation between two neighboring fields, in other words, terms like $\langle\left[\tilde{M}_{\rm ap}(\theta_{\rm c})\tilde{\mathcal{N}}(\theta_{\rm c})\right]_i\left[\tilde{M}_{\rm ap}(\theta_{\rm c})\tilde{\mathcal{N}}(\theta_{\rm c})\right]_{j\neq i}\rangle$ are neglected. This point is discussed at the end of this Appendix. Thus it is possible to express $\tilde{X}_{\theta_{\rm c}}$ as a function of the ensemble average $\langle X_{\theta_{\rm c}}\rangle$, and a random variable $E_{\theta_{\rm c}}$,

$$\tilde{X}_{\theta_{\rm c}} = \langle X_{\theta_{\rm c}}\rangle(1 + E_{\theta_{\rm c}}) \tag{A2}$$

where $\langle X_{\theta_{\rm c}}\rangle = \langle M_{\rm ap}(\theta_{\rm c})\mathcal{N}(\theta_{\rm c})\rangle$, and $E_{\theta_{\rm c}}$ is a random variable such that $\langle E_{\theta_{\rm c}}\rangle = 0$. The limit of small correlation $\langle X_{\theta_{\rm c}}\rangle \simeq 0$ is used, then the dispersion of $E_{\theta_{\rm c}}$ is $\langle E^2_{\theta_{\rm c}}\rangle = 1/(N_{\theta_{\rm c}}\mathcal{S}^2_{\theta_{\rm c}})$.

$\tilde{\mathcal{R}}$ was defined as

$$\tilde{\mathcal{R}} = \frac{\tilde{X}_{\theta_c}}{\langle \mathcal{N}^2(\theta_c)\rangle}\frac{\langle \mathcal{N}^2(1')\rangle}{\tilde{X}_{1'}}. \quad \text{(A3)}$$

We want to calculate the dispersion $\sigma^2_{\tilde{\mathcal{R}}} = \langle\tilde{\mathcal{R}}^2\rangle - \langle\tilde{\mathcal{R}}\rangle^2$. As explained in Sect. 4, the dispersion of the measurement of $\mathcal{N}^2$ is neglected, this is why ensemble average values $\langle\mathcal{N}^2\rangle$ comes directly in (A3). Provided that the number of fields is large, $N_{\theta_c} \gg 1$, the dispersion $\langle E^2_{\theta_c}\rangle$ is small compare to 1, thus the calculation of $\sigma^2_{\tilde{\mathcal{R}}}$ may be restricted to the second order in E_{θ_c}. In addition, neglecting the cross-correlation terms like $\langle E_{\theta_c} E_{1'}\rangle$ (this is discussed at the end of this Appendix), the dispersion of $\tilde{\mathcal{R}}$ is given by,

$$\begin{aligned}\langle\tilde{\mathcal{R}}^2\rangle &\simeq \frac{\langle\mathcal{N}^2(1')\rangle^2}{\langle\mathcal{N}^2(\theta_c)\rangle^2}\frac{\langle X_{\theta_c}\rangle^2}{\langle X_{1'}\rangle^2} \\ &\quad \langle 1 + E^2_{\theta_c} + 2E_{\theta_c} - 2E_{1'} + 3E^2_{1'} + ...\rangle \\ &= (1 + \langle E^2_{\theta_c}\rangle + 3\langle E^2_{1'}\rangle + ...), \end{aligned} \quad \text{(A4)}$$

and,

$$\begin{aligned}\langle\tilde{\mathcal{R}}\rangle^2 &\simeq \frac{\langle\mathcal{N}^2(1')\rangle^2}{\langle\mathcal{N}^2(\theta_c)\rangle^2}\frac{\langle X_{\theta_c}\rangle^2}{\langle X_{1'}\rangle^2}\langle 1 + E_{\theta_c} - E_{1'} + E^2_{1'} + ...\rangle^2 \\ &= 1 + 2\langle E^2_{1'}\rangle + ... \end{aligned} \quad \text{(A5)}$$

and finally,

$$\sigma^2_{\mathcal{R}} = \langle E^2_{\theta_c}\rangle + \langle E^2_{1'}\rangle = \frac{1}{N_{\theta_c}\mathcal{S}^2_{\theta_c}} + \frac{1}{N_{1'}\mathcal{S}^2_{1'}}, \quad \text{(A6)}$$

and the signal-to-noise of $\mathcal{R}$ is $1/\sigma_{\mathcal{R}}$. The derivation of (A6) implies some simplifications mentioned above, which have to be discussed. From a practical point of view, the N_{θ_c} fields should be extracted from one large survey (or at least, the largest scale of interest should be the smallest scale of a sub-field from a fragmented survey). Thus we expect that two neighboring fields are correlated and that two fields centered on the same position but with two different smoothing scales are also correlated. It has been shown in SvWJK (Fig. 8) that the use of compensated filters allows to neglect these correlations[5]; the aperture mass $M_{\rm ap}(\theta_c)$ of two neighboring fields of radius θ_c with a separation θ_c between the two centers are decorrelated by a factor of 10, and more than a factor 100 if the separation is $2\,\theta_c$. The aperture mass of two coincide fields with a factor of 5 between the two smoothing scales are also decorrelated by a factor of 10. Moreover, if these two fields are off-centered (which can be done in practice), the decorrelation is stronger. For example, two fields with a scale ratio of 2 are decorelated by a factor larger than 10 if they are off-centered by only half of the radius of the largest field. These decorrelation properties, direct consequences of the use of compensated filters, justify the assumptions made above to derive (A6).

[5] Even if the compensated filter used here is not excatly the same as in SvWJK, the decorrelation properties of this type of filter are the same.

References

Bardeen, J.M., Bond, J.R., Kaiser, N., Szalay, A.S., 1986, ApJ, 304, 15
Baugh & Gaztañaga, 1996, MNRAS 280, L37
Bernardeau, F., van Waerbeke, L. & Mellier, Y., 1997, A&A 322, 1
Blandford, R.D., Saust, A.B., Brainerd, T.G. & Villumsen, J.V.,1991, MNRAS 251, 600
Charlot, S., *private communication*
Fry, J.N. & Gaztañaga, E., ApJ, 1993, 413, 447
Jain, B & Seljak, U. 1997 ApJ 484, 560
Kaiser, N., 1992, ApJ 388, 272
Kaiser, N., 1996, astro-ph/9610120
Kaiser, N., Squires, G., Fahlman, G. & Woods, D., 1994, in: *Clusters of Galaxies*, eds. F. Durret, A. Mazure & J. Tran Thanh Van, Editions Frontieres
Miralda-Escudé, J., 1991, ApJ 380, 1
Moessner, R., Jain, B., 1997, astro-ph/9709159
Peacock, J.A. & Dodds, S.J., 1996, MNRAS 280, L19
Pelló, R., Miralles, J.M., Leborgne, J.F., Picat, J.P., Soucail, G., Bruzual, G., 1996, A& A, 314, 73
Sanz, J.L., Martinez-Gonzales, E., Benitez, N., 1997, astro-ph/9706278
Schneider, P., 1996, MNRAS 283, 837
Schneider, P., 1997, astro-ph/9708269
Schneider, P., van Waerbeke, L., Jain, B., Kruse, G., 1997, astro-ph/9708143 (SvWJK)
Tyson, J. A., 1988, AJ, 96, 1
Villumsen, J., 1996a, MNRAS 281, 369
Villumsen, J., 1996b, MNRAS *accepted*
Villumsen, J., Freudling, W. & da Costa, L., 1997, ApJ, 481, 578